

High power coupler development for EIC

W. Xu

July 2021

Electron-Ion Collider
Brookhaven National Laboratory

U.S. Department of Energy
USDOE Office of Science (SC), Nuclear Physics (NP) (SC-26)

Notice: This technical note has been authored by employees of Brookhaven Science Associates, LLC under Contract No. DE-SC0012704 with the U.S. Department of Energy. The publisher by accepting the technical note for publication acknowledges that the United States Government retains a non-exclusive, paid-up, irrevocable, world-wide license to publish or reproduce the published form of this technical note, or allow others to do so, for United States Government purposes.

DISCLAIMER

This report was prepared as an account of work sponsored by an agency of the United States Government. Neither the United States Government nor any agency thereof, nor any of their employees, nor any of their contractors, subcontractors, or their employees, makes any warranty, express or implied, or assumes any legal liability or responsibility for the accuracy, completeness, or any third party's use or the results of such use of any information, apparatus, product, or process disclosed, or represents that its use would not infringe privately owned rights. Reference herein to any specific commercial product, process, or service by trade name, trademark, manufacturer, or otherwise, does not necessarily constitute or imply its endorsement, recommendation, or favoring by the United States Government or any agency thereof or its contractors or subcontractors. The views and opinions of authors expressed herein do not necessarily state or reflect those of the United States Government or any agency thereof.

HIGH POWER COUPLER DEVELOPMENT FOR EIC*

Wencan Xu[†], J. Fite, D. Holmes, Z. Conway, K. Smith, A. Zaltsman
Brookhaven National Laboratory, Upton, USA, 11790

Abstract

The synchrotron radiation loss in EIC Electron Storage Ring is as high as up to 10 MW. This energy loss will be compensated by 17 2K 591 MHz single-cell SRF cavities with a combined total of 34 high power fundamental power couplers. Each power coupler will operate 92% of revolution time CW and ~8% of revolution time with 400 kW forward power due to the beam abort gap. To satisfy the EIC needs, we developed two 500 kW standing-wave FPC designs at BNL based on either a BeO and an Al_2O_3 RF window. This paper will briefly summarize test results of the BeO window FPC, and describe the design development of the Al_2O_3 window based FPC.

FPCS FOR EIC ESR SRF CAVITIES

The EIC operating scenarios has in a wide range of beam current and energy and scenarios [1], which demands a wide range of power and external Q variations. For each FPC, the power spans from 120 kW to 400 kW, and the variation of external Q is from $5.12\text{E}4$ to $7.15\text{E}5$. These FPCs are arguably one of the most critical and challenging components for the EIC RF/SRF systems. The concept design of EIC eSR SRF cavity cryomodule is shown in Figure 1 with the dual waveguide-fed couplers protruding horizontally from the cryomodule.

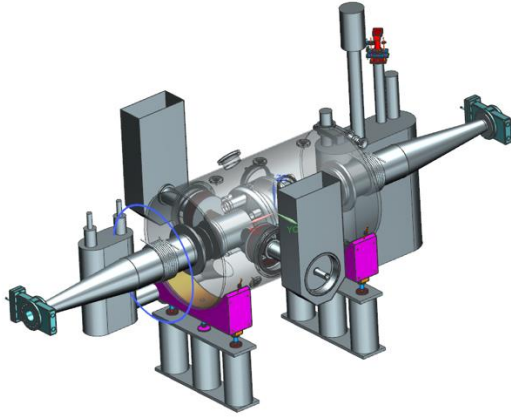


Figure 1: EIC eSR SRF cryomodule

The design and testing of the EIC FPCs is based upon the couplers operating with a 1 MW travelling wave or 500 kW standing wave, all phases. In the following sections we review EIC developments for the design and testing of a BeO RF window and a new design for an EIC acceptable Al_2O_3 RF window. This paper concludes with a

brief summary and comments on the future plans for this work.

BEO WINDOW FPC TEST RESULTS

Refurbished FPC conditioning test setup

The detailed design of the BeO window FPC tested here was described in [2]. These couplers have been used for operation in R&D ERL [3] and LeREC booster SRF cavity [4], although the power level was much lower than designed 1 MW. In 2018, we decided to test the BeO window FPCs but up to EIC operating power level, i.e., MW level. The primary test goal was to verify the power handling capability of these coupler. So, several improvements were done in 2019, prior to high power test.

- Upgraded the 704 MHz klystron to allow output power close to 1 MW.
- Reviewed and recalculated all the RF-thermal simulation of the FPCs and conditioning box.
- A pair of BeO window FPC were fabricated by CPI. We increased the size of water cooling channel in FPC airside outer conductor, and change braze-joint instrumentation port to tig-weld joint.
- Refurbished FPC conditioning setup, interlock, data logging.

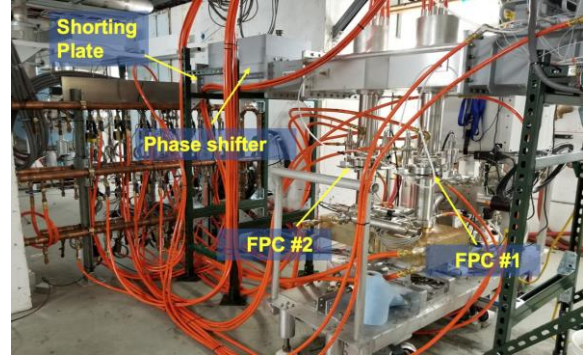


Figure 2: BeO window FPC test setup

BeO FPC high power test results

A pair of BeO RF window based FPCs were tested with a standing wave at 704 MHz in early 2020, the test setup is shown in Figure 2. FPC conditioning proceeded in stages to accurately gauge coupler performance with forward power levels set at 100, 200, 300, 400, and 500 kW. At each power level the conditioning started with a low duty cycle, short pulse (1 μs) and ended up CW. Once CW operation at each level was achieved the reflected RF phase was varied in 10 degree increments over 80 degrees (limit of the high-power phase shifter) and the conditioning process was repeated before increasing the RF power to the next higher level. The highlights of test results are listed as followings.

* This work is supported by Brookhaven Science Associates, LLC under Contract No. DE-SC0012704 with the U.S. Department of Energy.

[†] wxu@bnl.gov

- The BeO window FPCs were successfully conditioned to 400 kW, CW, standing wave, all phases, with no troubles detected with vacuum, arc, or thermal sensors.
- At the first phase of 500 kW conditioning, the FPCs were successfully operated with a 500 kW CW standing wave.
- After the first phase of 500 kW conditioning, the phase was shifted by 10 degrees and the pulse conditioning proceeded to 500 kW. However, one BeO window cracked when the cw power reached 480 kW CW.

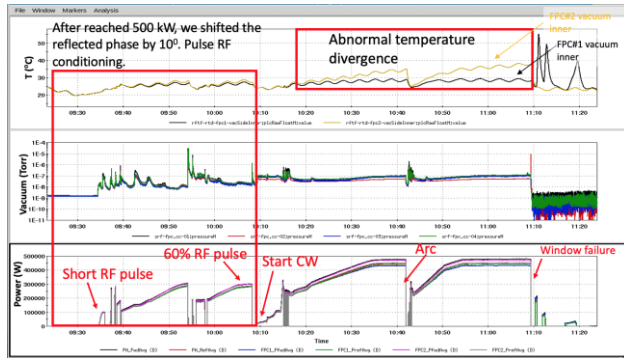


Figure 3: FPC conditioning prior to window failure at 480 kW, CW, standing wave.

As shown in Figure 3, some conditioning/vacuum activity was observed. After the pulsed duty cycle reached 60 %, CW conditioning started. CW conditioning at the second phase reached 480 kW where substantial vacuum activity and arcing occurred. It was also observed that the temperature difference between the two FPCs' vacuum side inner conductors diverged. After about 30 minutes at 480 kW, one BeO window cracked.

Investigation of window failure

After the BeO RF window cracked and vented the coupler vacuum space, the system was disassembled and inspected. It is interesting to note that several of the BeO RF window cracks aligned well with marks observed during receipt inspection, Figure 4. It is speculated that intrinsic defects in the BeO RF window led to early breakdown. Conclusions here are complicated by a close investigation of the conditioning data in Figure 3 and comparing to the arcing marks shown in Figure 5 and the air-side arc detector location highlighted in Figure 6 (Top). Correlating all of these observations leads to the conclusion that there were arcs on the airside missed by the air side arc detector. As shown in Figure 6 (Top), the air-side arc detector was located on the half height WR1500 waveguide about 22 cm away from the doorknob transition. The distance between doorknob and BeO window is 50 cm with a 90 degree turn between the waveguide arc detector locations and the FPC's RF window. This geometry precludes direct line-of-sight observation of air-side RF window arcs and arcs occurring on the far-side of the doorknob transition, which certainly occurred during conditioning. In the future two 5

mm diameter holes will be added on the airside outer conductor flange, one hole for the arc detector and the other for dry air flow to flush out ozone and other arcing gas by-products.

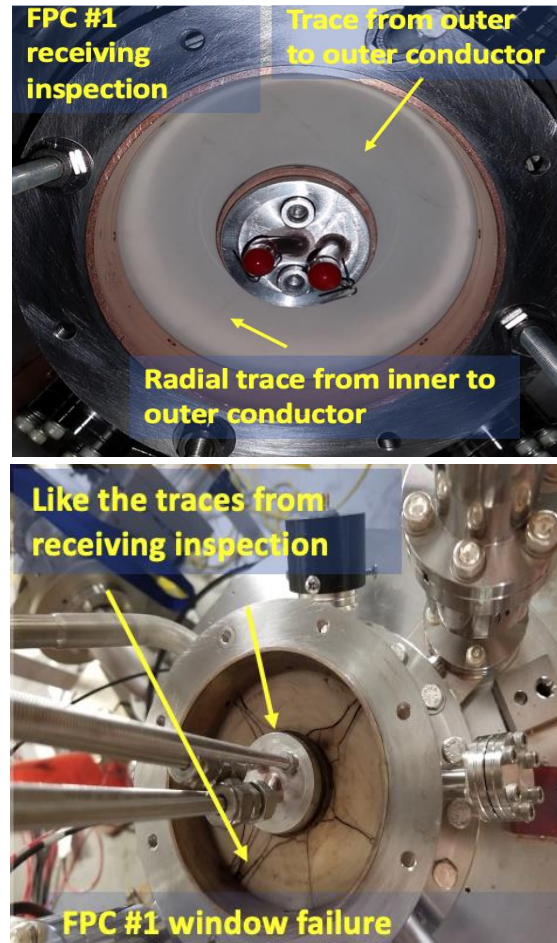


Figure 4: Various marks on BeO window observed in receiving inspection (Top); BeO window cracks.



Figure 5: Arc mark in the FPC#1 airside.

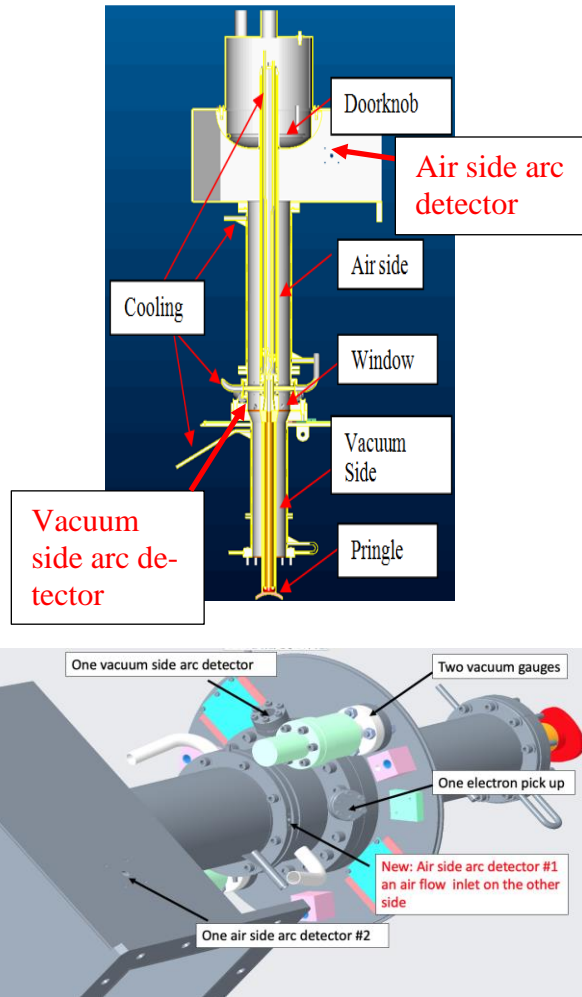


Figure 6: Original air side arc detector (Top); Added an arc detector near window, and a venting hole for dry air flow (Bottom).

DESIGN OF A NEW MW ALUMINA FPC

While BeO demonstrated feasibility of operating the coupler at EIC power levels (proof of principle), two factors have driven the development of an alternative: (1) strick safety regulations on handling BeO dramatically slow down all handling and the window's mechanical strength appears insufficient for transportation of an assembled cryomodule over long distances. The reason for using BeO for MW FPC design more than a decade ago was because of its low loss tangent and higher thermal conductivity compared to 96% alumina, with the trade-off being BeO's lower mechanical strength. In the past decade, technology of brazing high purity alumina (99.5%) becomes mature and reliable, and it has a factor of 4 lower loss tangent than BeO, with mechanical strength better than 96% alumina. To benefit from the development of this technology, we decided to development a 99.5% alumina based MW RF coupler.

Considerations for alumina window FPC design

The physics design consideration of RF window optimization includes lower normal components of electric field near the window to reduce potential multipacting electron striking on window, maintain a reasonable total peak field around the braze joint and choke, less multipacting zones in the coaxial line and better coupling to meet the EIC low Q_{ext} requirement. While not compromising physics performance, engineering consideration for coupler design is crucial for application, such as requirement from road trip (5 g impact load from any direction), quality assurance of TiN coating, and ease of inspection.

Figure 7 compares the BeO window FPC and new alumina RF window designs with vacuum side inner conductors. The changes between the 2 designs are colour coded, and they are listed as following. a). the window thickness was increased from 6.3 mm to 10.1 mm to increase the mechanical strength of the window; b). the choke to window distance was increased from 3 mm to 10.1 mm for better access for TiN coating and inspecting window-copper sleeves braze joint; c). inner diameter of window was increased from 22.5 mm to 28 mm to reduce the peak RF surface fields on the inner conductor and to increase the mechanical strength; d). the diameter of FPC's 50 Ω transmission line was increased to push multipacting zones to higher power levels and increase the coupling to the cavity (EIC needs Q_{ext} as low as $5e4$).

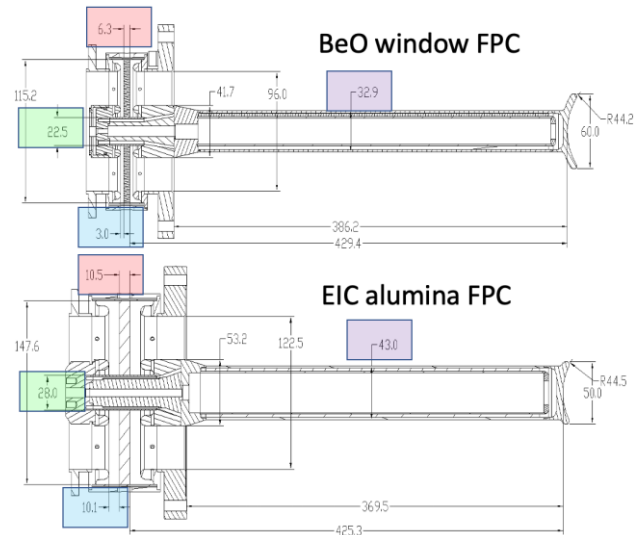


Figure 7: FPC window assembly: BeO window FPC (Top) and new alumina FPC (Bottom).

RF performance

CST Microwave Studio calculations [5] of the new alumina RF window design's S_{11} is shown in Figure 8. This is a broadband window, as its S_{11} is smaller than -30 dB for frequencies < 820 MHz, because of this we plan to use the same alumina RF window on other EIC RF/SRF systems. The maximum electric field in the window assembly is 717 V/m per 0.5 W average traveling wave. This peak surface field occurs on the outer surface of the inner

conductor choke. The peak field at the ceramic-copper braze joint is 260 V/m (per 0.5 W travelling wave). Scaling these fields to the test criteria of the EIC eSR SRF cavity's FPC, i.e 1 MW average power, its fields are lower than other high power couplers in test, Figure 9.

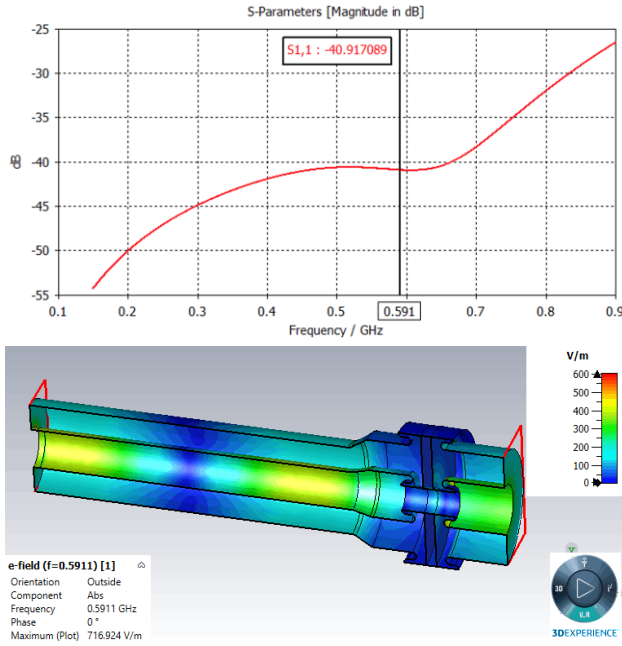
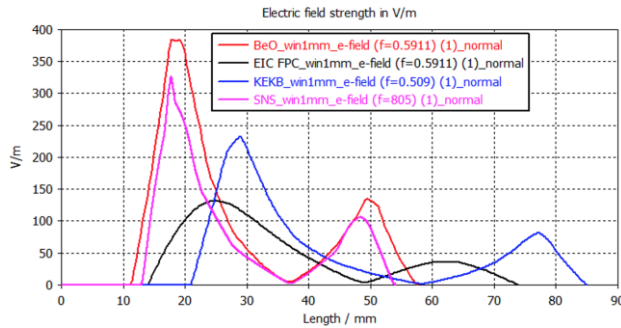
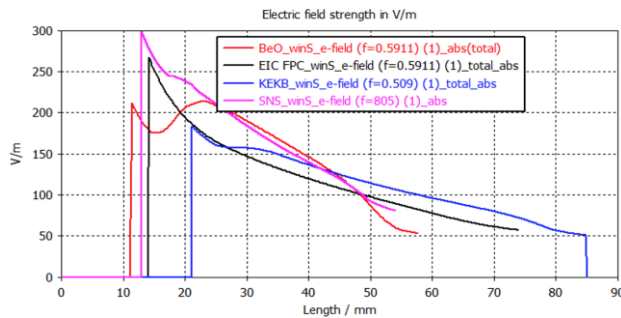


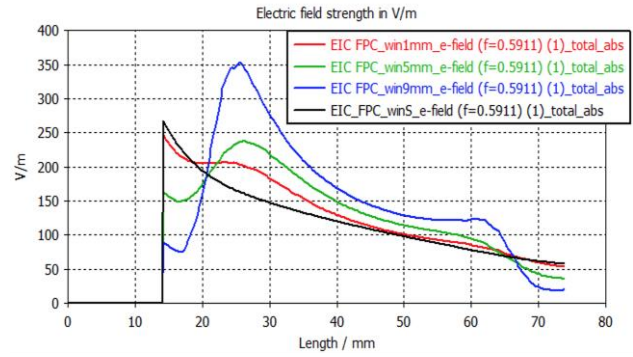
Figure 8. S11 of new window design (Top) and field profile of window assembly.



(a). Electric normal (to window surface) component at 1 mm away from window surface, along radius (horizontal axis)



(b). Absolute Electric field on the surface of window along radius (horizontal axis)



(c). Absolute field at various distances away from window surface

Figure 9. Field near RF window.

Multipacting simulation

Multipacting simulations were carried out with SPARK3D [6]. Two multipacting regions were studied so far: (1) the coaxial line between the RF window and cavity beam pipe and (2) the coaxial region around the RF window, Figure 10. Several distinct multipacting scenarios were studied in these two regions covering several select forward power levels, different levels of surface SEY and the effects of DC bias.

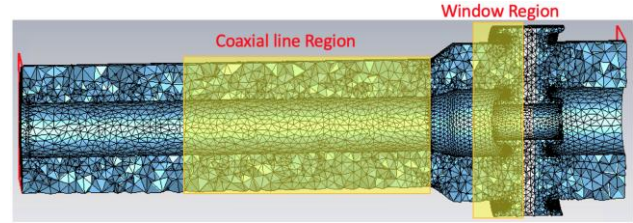


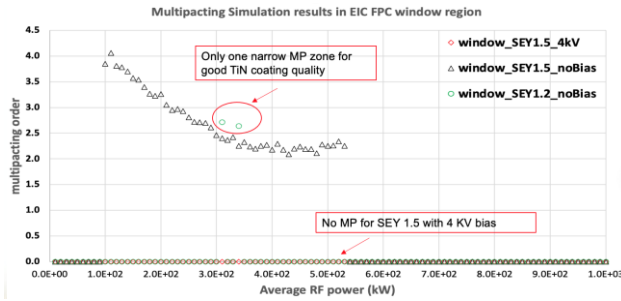
Figure 10. Multipacting simulation regions

The SEY parameter of TiN depends on the coating quality. A reasonable peak SEY for TiN is between 1.2 – 1.5 and results with varying TiN SEY are summarized in Figure 11. When good TiN coating SEY is used, there is one single narrow multipacting zone around 310 kW (TW) over the entire range of relevant EIC RF power levels from 0 to 1 MW. This is not surprising because the normal component of the electric field was optimized to reduce potential multipacting electrons striking the RF window. In this case, most likely, we would condition through the multipacting zone, and no bias is needed. If the TiN coating quality is poor, the number of multipacting zones increases. The entire range of multipacting can be suppressed with a 4 kV DC bias applied between center and outer conductor.

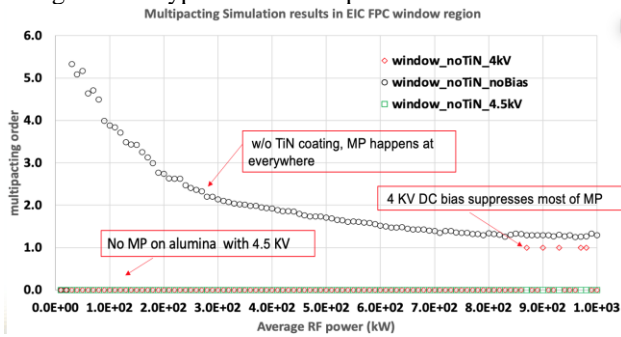
The extreme case for multipacting is shown in Figure 11(b), i.e, when there is no TiN coating at all on the window surface, here the maximum SEY is as high as 9 and $SEY > 1$ for all impact energies above 20 eV. It is not surprising that multipacting ranges over the all EIC operating levels. However, this study shows that all multipacting will be suppressed with a 4.5 kV DC bias.

Multipacting results for the coaxial line are shown in Figure 11 (c) and again a 4.5 kV DC bias suppresses all

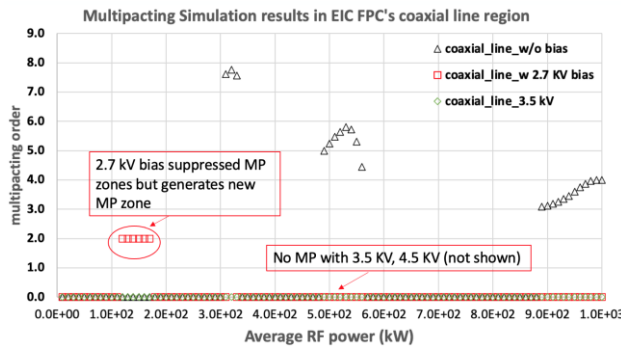
multipacting. Based upon these results the EIC coupler design will include a provision for a 4.5 kV DC bias, just in case. However, this doesn't mean to alleviate pursuing high quality TiN coating, as it also reduces the discharge time of electrons (if there is any) landing on the window.



(a). Multipacting simulation results in window region with typical TiN SEY parameters



(b). Multipacting simulation results in window region w/o any TiN coating



(c). Multipacting simulation results in coaxial line region

Figure 11. Multipacting simulation results

RF-Thermal analysis

RF loss for thermal analysis were calculated with HFSS [7] and cross-checked with CST. The HFSS RF losses were imported into ANSYS for thermal-mechanical calculations. The RF loss is based on a 1 MW average power, travelling wave. The water-cooling channel's film coefficients were calculated (conservatively) and applied separately. The RF window and choke area temperature results are shown in Figure 12. The ΔT within the ceramic is only 10 C from 24 to 34 C, and the choke tip has the highest temperature at 34 C.

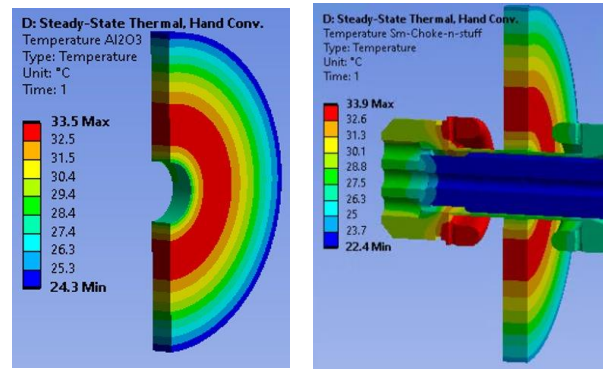


Figure 12. Temperature profile on RF window (left) and choke area (right)

Mechanical analysis

Mechanical analysis was carried out with the same boundary conditions expected when the FPC is shipped after installation on a cavity in a cryomodule. In this configuration a 5g load in all directions was applied to simulated the shock loads projects in [8]. Figure 13 shows the boundary conditions: flange on the outer conductor is mounted to cryomodule, and airside inner conductor is fixed with special tooling. Simulation results show that with a vertical 5g load the inner conductor tip only deflects 0.0073 inches and the maximum elastic copper strain is 0.0003 in/in. The stresses are all below expected material yield. Mechanical modal analysis with the same boundary condition found the first mechanical mode frequency to be 100 Hz, which is well above typical transportation excitation frequencies of ~ 10 Hz and the utility frequency ~60 Hz found in operation.

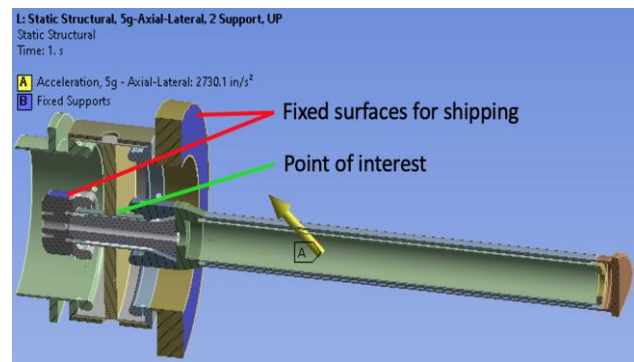


Figure 13. Boundary condition for mechanical simulation

SUMMARY AND PLAN

EIC eSR SRF cavity requires the FPCs to handle up to 1 MW power levels. BeO RF window based FPCs were tested and demonstrated feasibility of operating at 1 MW. Based on experience with the BeO RF window FPC and other FPCs deployed around the world, a robust, broadband alumina FPC window was designed. Detailed RF, thermal, mechanical, multipacting study were carried out

on the new FPC. The new alumina RF window design will be prototyped and tested in the future.

ACKNOWLEDGEMENT

The authors would like to thank the following people for fruitful and interesting discussions Robert Rimmer, Jiquan Guo, Jim Henry, Frank Marhouser from Jlab.

REFERENCES

- [1] EIC Concept Design Report, https://www.bnl.gov/ec/files/EIC_CDR_Final.pdf
- [2] W. Xu *et al.*, “Design, simulations, and conditioning of 500 kW fundamental power couplers for a superconducting rf gun”, in *Phys. Rev. ST Accel. Beams* **15**, 072001.
- [3] W. Xu *et al.*, Beam Commissioning of the SRF 704 MHz Photoemission Gun, the 6th International Particle Accelerator Conference (IPAC’15)
- [4] W. Xu *et al.*, “Commissioning of the SRF Booster Cavity for LEReC”, Proceedings, 29th Linear Accelerator Conference, LINAC2018 : Beijing, China, 16-21 September 2018.
- [5] CST, <https://www.3ds.com/products-services/simulia/products/cst-studio-suite/>
- [6] Spark 3D, <https://www.3ds.com/products-services/simulia/products/spark3d/>
- [7] HFSS, <https://www.ansys.com/products/electronics/ansys-hfss>
- [8] T. Whitlatch *et al.*, “Shipping and alignment for the SNS cryomodule”, Proceedings of the 2001 Particle Accelerator Conference, Chicago